Proceedings World Geothermal Congress 2026
Calgary, Canada, June 8 – 11, 2026

A Geosystem-Integrated Strategy for Optimizing Deep Geothermal Development in the Middle Upper Rhine Region: The DEKAPALATIN-BERTHA Project

E. Meneses Rioseco[1]*, G. Lee Exuzian[1], M. O. Abdelmoula[1], D. Ravidà[1] and I. Moeck[1,2]
[1]Georg-August Universität Göttingen, [2]LIAG-Institute of Applied Geophysics
(*) ernesto.menesesrioseco@uni-goettingen.de

Keywords: Deep geothermal energy, Upper Rhine Graben, reservoir modeling and reservoir simulation, heat anomaly, topography-driven flow (forced convection), density-driven flow (natural convection), reservoir potential assessment.

ABSTRACT

The Upper Rhine Graben in Germany is a notable, recent, regional example of the most dynamic advancements in the deployment of deep geothermal energy in Central Europe. However, the region is still dominated by district heating networks primarily fueled by fossil energy sources. Geothermal energy presents significant potential to substitute coal and natural gas in these systems, positioning the region as a strategic focal point for advancing the thermal energy transition in Germany. This work presents the recent progress in the joint research project DEKAPALATIN-BERTHA, which is located in Wörth am Rhein, in the Middle Upper Rhine (MUR), Germany. The MUR region may represent a fault-leakage controlled play, whose fault inventory and hydraulic performance are insufficiently understood. The safe development of this type of play requires a targeted exploration strategy supported by high-quality data and dynamic modelling and simulation. To mitigate the risks associated with geothermal exploration and development, this study investigates subsurface heat transport processes with the objective of identifying and quantifying key interdependencies and controlling factors. A central focus is the development and application of advanced dynamic predictive modeling approaches tailored to fracture- and fault-controlled geothermal reservoirs. To enhance the understanding and forecasting of reservoir behavior under various operational scenarios, multi-scale and interdisciplinary datasets are integrated into coupled thermo-hydro-chemical (THC) numerical simulations. Besides, combined sedimentological-petrophysical analyses and log-correlations offer an integrated framework that significantly strengthen the assessment of medium-deep geothermal potential. We present our recent progress, mainly focusing on the modelling and simulation part.

1 INTRODUCTION

Geothermal energy is a promising renewable resource with the potential to contribute significantly to sustainable energy supplies worldwide (Kassem and Moscariello 2025). Its viability heavily depends on successful exploration concepts, availability and integration of existing multi-scale and multi-disciplinary data as well as on the long-term stability and sustainability of geothermal reservoir performance under envisaged operational conditions. In particular, the successful use of low-enthalpy geothermal energy for heating purposes relies on overlapping aspects such as high geothermal energy potential, high heat-demand and the existence of favorable infrastructures (e.g., district heating network) (see Moeck et al. 2026 in this volume).

Geothermal resources can play a pivotal role in accelerating Germany's *Energiewende* by providing low-carbon, baseload heat for buildings, industrial processes and district heating networks, thereby addressing the particularly fossil-fuel-intensive heating sector. Recent assessments of Germany's deep geothermal resources indicate substantial technical potential for space, industrial processes and district heating, suggesting that expanded deployment could significantly contribute to long-term decarbonization targets (Agemar et al., 2014).

The Upper Rhine Graben (URG) in Germany stands out as one of the most prominent and recent examples of rapid progress in deep geothermal energy development within Central Europe (e.g., Frey et al. 2022). Despite this momentum, district heating networks across the area continue to rely largely on fossil-based fuels. Harnessing geothermal resources offers considerable opportunities to replace coal and natural gas in these systems, making the region a key target for driving Germany's transition toward sustainable thermal energy. One recent initiative that exemplifies this objective is a collaborative effort involving the municipality of Wörth am Rhein together with industrial partners Daimler Truck and EnBW, supported by the academic and research institutions of the University of Göttingen, TU Darmstadt, IGEM, and LIAG-Institute, e.g., Moeck et al. 2026 in this volume. The consortium seeks to realize a comprehensive geothermal heating project, guiding it through all stages of development as an integrated showcase

located within one of Germany's most significant geothermal anomalies (see Fig. 1). Conceived as a real-world laboratory, the initiative will be carried out directly at the Wörth am Rhein site, enabling practical testing and demonstration under authentic operating conditions. Taken together, these activities form the DEKAPALATIN-BERTHA joint research project, located in Wörth am Rhein within Germany's Middle Upper Rhine (MUR) region.

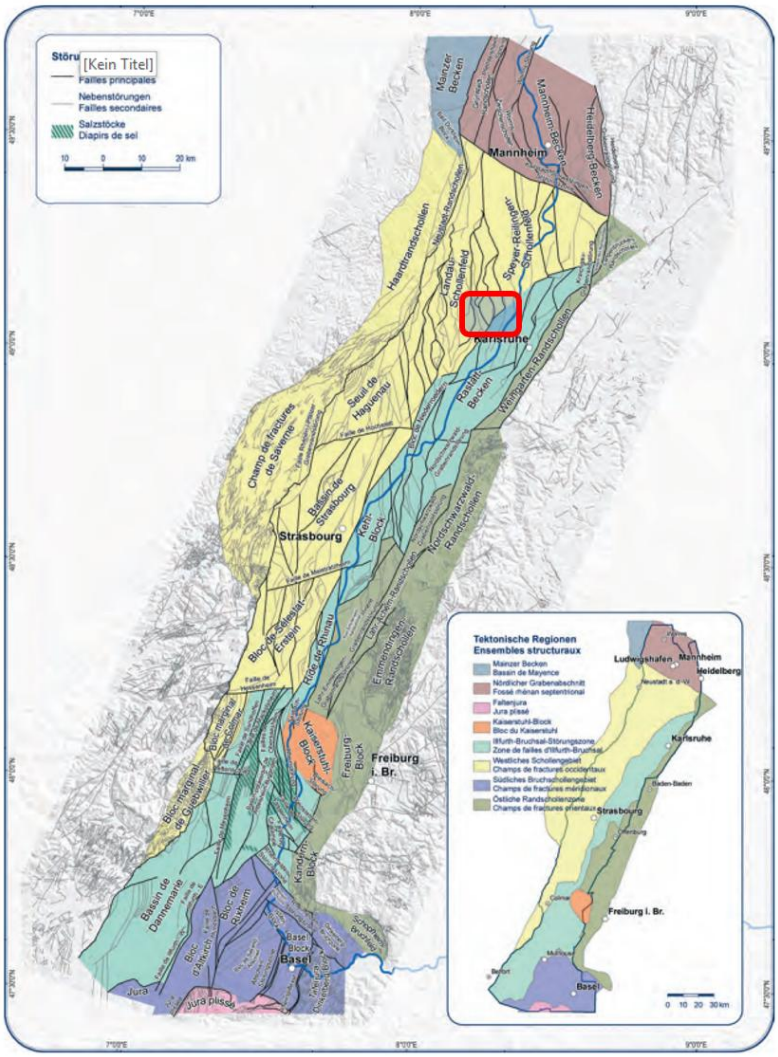


Figure 1. Structural map of the Upper Rhine Graben showing major lineaments and outcropping geological units, modified after GeORG-Projectteam (2013). The study area, including Wörth am Rhein near Karlsruhe, is highlighted by the red rectangle.

The Upper Rhine Graben (URG) represents an active rift system and corresponds to an *extension play type* in Moeck's (2014) geothermal play-type framework. Its rift-related high heat flow, together with networks of permeable normal faults, promotes geothermal energy utilization by enabling large-scale groundwater circulation driven by topographic gradients and/or buoyancy effects (e.g. Clauser and Villinger 1990, Pribnow and Schellschmidt 2000, Clauser et al. 2002, Vallier et al. 2019). The interplay of intricate fault systems with a heterogeneous stratigraphic architecture produces a highly variable permeability distribution, which—when combined with regional groundwater flow—strongly influences local thermal anomalies and the performance of geothermal reservoirs. Operational experience from geothermal installations in the URG further demonstrates the occurrence of highly saline formation fluids, particularly within key target units such as the Muschelkalk, the Middle Buntsandstein, and the crystalline basement (Sanjuan et al. 2010, 2016).

A better understanding of the governing factors behind these observations—and their interactions—through the integration of multi-scale geoscientific datasets in geological and numerical subsurface models can help reduce geothermal exploration risk and improve predictions of fault- and fracture-controlled reservoir behavior. Building on a systematic compilation and synthesis of published data, this study focuses on numerical modeling and simulation of thermo-hydraulic (TH) and thermo-hydro-chemical (THC) processes, both conservative and reactive, across multiple spatial and time scales. Here, we present our most recent advances toward this objective.

2 SUBSURFACE REGIONAL MODEL

The GeORG initiative arose from a transnational research effort under the Interreg IV Upper Rhine project. Over roughly four years, partners from Germany, France and Switzerland assembled and harmonized extensive geological, seismic, borehole and geophysical data across the URG to build the first comprehensive three-dimensional geological model of the basin down to several km depth (GeORG-Projektteam 2013). With a model volume of approximately 270 × 50 × 6 km, the GeORG model provides a unified subsurface framework for assessing deep-geological potentials — including deep geothermal energy, thermal waters, and in general subsurface energy reservoirs — thus supporting both resource exploration and sustainable subsurface planning in the URG. However, it should be noted that, because the model is constrained by relatively sparse data, its resolution varies spatially and is generally coarse in several areas.

As the foundation for our regional and reservoir-scale thermo-hydraulic modeling and simulation, we extract a subsection of the structural and stratigraphic GeORG model that encloses the study area (Fig. 1) and spans roughly 17 × 17 km laterally, extending to a depth of about 7 km. To be able to transform this 3D subsurface model, which was originally built for observational purposes, into a model capable of handling finite-element dynamic thermal-hydraulic simulations, we use the structural and stratigraphic workflow and further processing operations in Aspen SKUA® until we get a “watertight” model that is geologically consistent and avoid self-intersections (see Fig. 2 and Fig. 3).

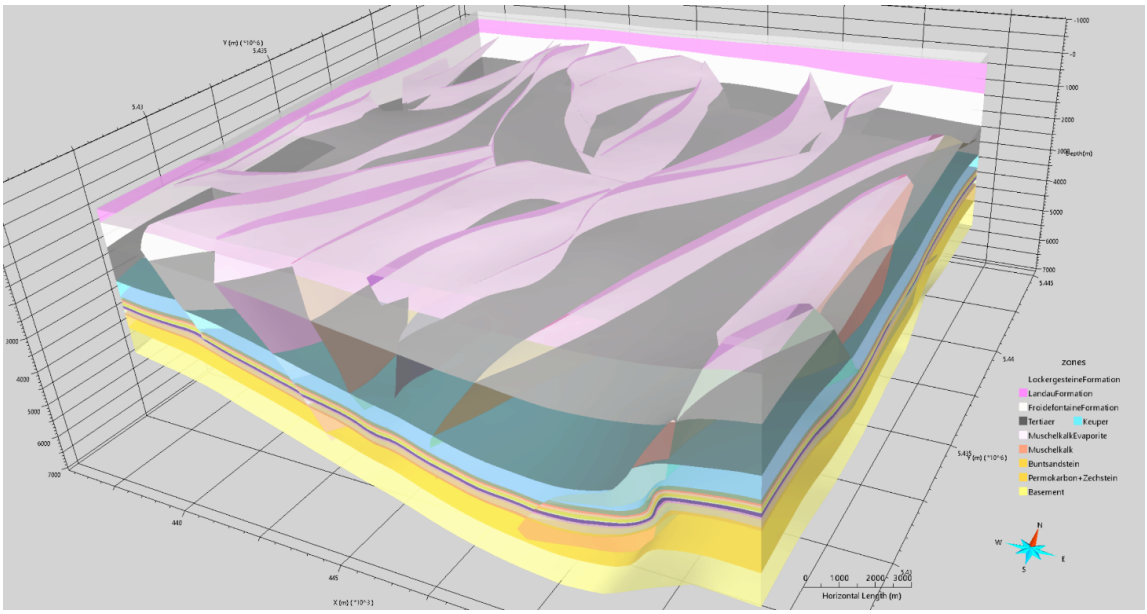


Figure 2. 3D subsurface model derived from the GeORG framework, covering approximately 17 × 17 km laterally and extending to a depth of 7 km. Additional stratigraphic refinement was incorporated within the Muschelkalk and Buntsandstein units. The model was constructed using Aspen SKUA®.

The stratigraphic framework of the study area within the Upper Rhine Graben (URG) consists of a crystalline basement overlain by a several kilometers thick and multilayered sedimentary successions. From top to bottom, Quaternary (glacio-)fluvial sands, gravels, and lacustrine deposits overlie clay-dominated marine to fluvio-marine Tertiary sediments, which in turn rest unconformably on Jurassic to Triassic and Late Paleozoic sedimentary units lying above the crystalline basement.

The shallow Cenozoic sediments host the principal near-surface aquifers of the URG and generally exhibit hydraulic properties conducive to substantial groundwater storage and flow. Historically, Oligocene and Miocene sandy bodies within the Pechelbronn Formation (Priabonian–Rupelian), the Niederrödern Formation (Chattian) and the *Melette Schichten* (Rupelian) have demonstrated excellent reservoir quality, as evidenced by their role in hosting significant hydrocarbon resources in the region (Reinhold et al., 2016). Though, some of these bodies are locally restricted and occur as lenses with limited lateral extent.

Among the Mesozoic formations, the Keuper sequence of the Germanic Triassic is dominated by marls, evaporites, and claystones with generally low permeability and therefore act as an effective barrier to vertical groundwater exchange (Koltzer et al., 2022). In contrast, the Middle Triassic Muschelkalk constitutes one of the most significant deep aquifers in the region. This unit, composed predominantly of fractured and locally karstified limestones and

dolomites, offers high transmissivity and considerable storage capacity, making it a frequent target for deep geothermal exploitation due to the favorable temperature and hydraulic conditions encountered at depth.

Other key reservoir unit belong to the Lower Triassic Buntsandstein Group, consisting of thick fluvio-aeolian to lacustrine successiond formed several hundred meters thick sandstone sequences occasionally interbedded with thin fine-grained clay deposits. The Buntsandstein is traditionally tripartite into Lower, Middle and Upper sub-groups. The middle Buntsandstein can be further differentiated into the Volpriehausen, Detfurth, Hardegsen, and Solling formations, following the stratigraphic interpretations derived from the nearby Waldbronn–Reichenbach II borehole. Because our goal is to perform thermo-hydraulic modeling and simulation at both regional and reservoir scales, it is necessary to construct a purpose-built hydrogeological model. To achieve an appropriate hydrostratigraphic representation, the lithostratigraphy was refined within the key hydrogeological units—the Muschelkalk and Buntsandstein formations—and especially within the Middle Buntsandstein, where additional stratigraphic horizons were introduced.

At the base of the sedimentary succession lie the Permo-Carboniferous (Rotliegend) units and the crystalline basement of the Saxothuringian domain. These rocks—primarily igneous and metamorphic—possess very low primary porosity and permeability and are thus treated as homogeneous units in the model. Nonetheless, secondary permeability associated with fracturing, particularly in the vicinity of major fault structures, can locally permit appreciable groundwater flow.

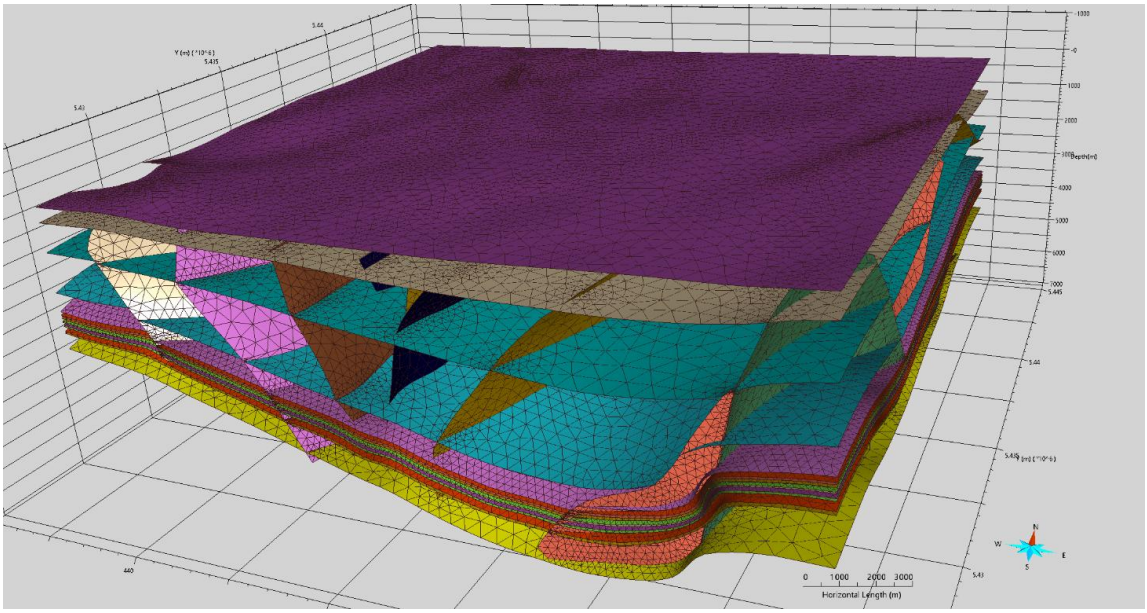


Figure 3. Triangulated fault and horizon surfaces of the 3D model after extensive reprocessing in Aspen SKUA®, with particular refinement at fault–fault and fault–horizon intersections to produce a geologically consistent, fully "watertight" model free of self-intersections.

The processed 3D subsurface model shown in Fig. 3 provides the foundation for both the subsequent 2D regional thermo-hydraulic simulations—aimed at elucidating the controls on the anomalously high temperatures in the MUR—and the 3D reservoir-scale thermo-hydraulic simulations performed on a smaller domain extracted from the larger model.

The thermal and hydraulic parametrization is based on values reported in the published literature (e.g., Frey et al. 2022, Freymark et al. 2017, Koltzer et al. 2019, 2022), as will be discussed later. Although this study concentrates on the Mesozoic formations—identified as key targets for deep geothermal exploitation within the DEKAPALATIN-BERTHA project—by examining their thermo-hydraulic behavior under various operational scenarios and their role in the observed anomalously high temperatures, the project also aims to assess medium-depth geothermal resources. In particular, several Tertiary units, including the Upper and Lower Pechelbronn formations and the Bunte Niederröderner layers, may offer additional geothermal potential and will be investigated in greater sedimentological detail in subsequent work (see, e.g., Reinhold et al. 2016). Accordingly, a more refined lithological and hydrostratigraphic representation will be incorporated into the model in future stages prior to drilling to more accurately evaluate the technical middle-deep geothermal potential. The petrophysical parametrization will additionally be informed by values reported from nearby hydrocarbon exploration (e.g., Böcker et al. 2017).

Ultimately, the current 3D model will be updated and validated following the drilling operations planned within the DEKAPALATIN-BERTHA project.

3 PHYSICO-CHEMICAL BACHGROUND AND COMPUTATIONAL FRAMEWORK

To evaluate the controlling mechanisms of the local heat anomaly and to forecast reservoir behavior under different injection–production scenarios, it is necessary to simulate coupled flow in fractured and porous media together with heat transport processes under a range of boundary-condition configurations. For the thermo-hydraulic simulations, we use the commercial finite-element software COMSOL Multiphysics®. The platform solves the governing partial differential equations (PDEs) through spatial and temporal discretization schemes, addressing mass, momentum (Darcy flow), and energy conservation (advection-diffusion equation) within a coupled system defined over the entire model domain. In this study, we assume transient conditions to capture natural convection processes via different equation of states (EoS), see e.g., Guillou-Frottier et al. 2013, 2020; Abreu-Torres et al., 2025 and references therein. Accordingly, the numerical framework solves the groundwater-flow equation derived from the coupling of the continuity equation with Darcy's law extensively described in the related literature, bidirectionally coupled with the energy equation (e.g. Magri et al. 2009).

In addition, the geothermal energy production heavily depends on the long-term stability and sustainability of geothermal reservoirs, which are often affected by mineral reactions such as dissolution and precipitation under operational conditions. These processes can alter the permeability, porosity, and overall integrity of the reservoir, leading to operational challenges such as mineral scaling, clogging of fractures, and reservoir souring (Diamond and Alt-Epping 2014; Yanaze et al., 2019). In fractured geothermal reservoirs, especially those involving complex mineralogy, these reactions are influenced by thermodynamic conditions, fluid composition, and temperature gradients, among other factors.

To realistically represent fully coupled thermo–hydro–chemical (THC) processes using globally validated hydrochemical databases, we employ an integrated computational framework comprising three software components: COMSOL Multiphysics®, iCP (interface COMSOL–PHREEQC; Nardi et al. 2014), and PHREEQC (Appelo and Postma 2005). Both equilibrium and kinetic reaction approaches are considered. The governing reactive transport equation has been extensively documented in the literature (e.g., Appelo and Postma 2005, Xiao et al. 2018).

3.1 Parametrization - Initial and boundary conditions

The volumetric parametrization of the regional model is based on a compilation of published data (Tab. 1; e.g., Frey et al. 2022; Freymark et al. 2017; Koltzer et al. 2019, 2022, and references therein). As illustrated in Fig. 4, each stratigraphic layer is treated as homogeneous, and the initial temperature field is derived from the 3D GeotIS dataset using Kriging interpolation (e.g., Agemar et al. 2012). A hydrostatic pressure gradient is also imposed.

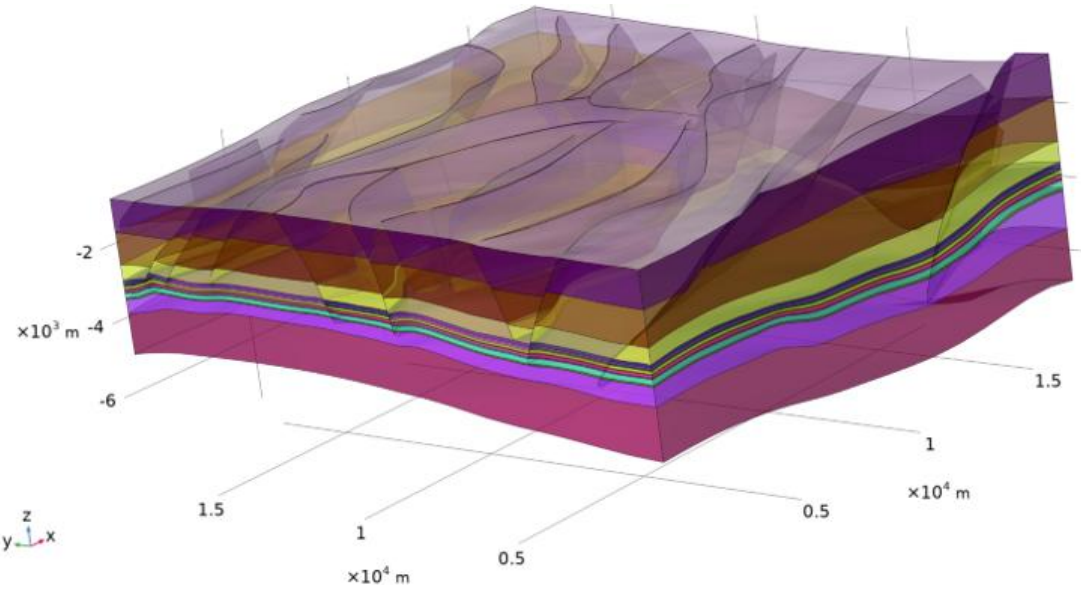


Figure 4. 3D parametrization of the regional model. Different colors indicate distinct thermal and hydraulic parameter sets, with each stratigraphic layer treated as homogeneous. Fault planes were assigned specific parameterizations, and key target faults were additionally volumetrized to incorporate a fault damage zone (FDZ) with an anisotropic permeability structure.

Table 1. Thermal and hydraulic rock parameters used in the 2D vertical cross sections, simplified 3D models, and the 3D reservoir model. Parameter values were compiled from GeORG-Projektteam 2013, Frey et al. 2022, Freymark et al. 2017, Koltzer et al. 2019, 2022 and references therein.

Formation	Poro [frac]	Perm [m^2]	Thermal Cond. [$W.m^{-1}K^{-1}$]	Heat Capacity [$J.kg^{-1}K^{-1}$]
Lockergesteine	0.35	1e-12	1.5	850
Landau	0.18	7e-14	2	915
Froidefontaine	0.18	7e-14	2	915
Tertiary	0.18	7e-14	2	915
Keuper	0.04	4e-16	2.2	800
Evaporite Muschekalk	0.01	1e-20	5.4	840
Muschelkalk	0.05	6e-14	3.25	700
Upper Buntsandstein	0.1	8e-15	2.8	680
Middle Buntsandstein	0.1	3e-14	2.8	680
Lower Buntsandstein	0.1	8e-15	2.8	680
Permo-Carbon	0.07	2e-15	2.1	735
Basement	0.01	3e-18	2.9	780

The boundary conditions were modified across the different model scenarios for several reasons. Although they were explored over a broad range of plausible configurations to assess how variations influence the thermal field and fluid-flow patterns within the study area, a set of general assumptions was maintained throughout. Atmospheric pressure is imposed as a Dirichlet boundary condition at the model surface, whereas the lateral and basal boundaries are specified as no-flux Neumann conditions. To represent topography-driven groundwater flow originating from the graben shoulders, a constant hydraulic head of 200 m is prescribed within the shallow reservoir on the eastern side of the model, following the concept described by Clauser and Villinger (1990).

Thermal boundary conditions are defined as follows: the upper surface is held at a constant temperature of 10 °C, and the model base, corresponding to the crystalline basement, is assigned a uniform heat-flux boundary of 100 mW m^{-2} in accordance with Lemgruber-Traby et al. (2023). Lateral boundaries are treated as thermally open, with inflow temperatures set according to the regional geothermal gradient.

3.2 Finite-Element numerical discretization and solver

Given the structural complexity of the model, characterized by numerous faults and tilted stratigraphic units, several fully unstructured finite-element meshes with localized refinement in areas of high thermal or hydraulic gradients were generated to identify an optimal 3D discretization. Such an optimal mesh provides sufficient resolution in zones where strong gradients occur, while being coarsened elsewhere to minimize the total number of elements and thus reduce computational cost (see e.g., Fig. 5). The mesh was also progressively coarsened toward regions of lesser interest, and care was taken to keep element distortion to a minimum throughout the domain.

In our thermo-hydraulic simulations, time discretization was carried out using COMSOL Multiphysics' implicit, variable-time-step scheme, which adapts the step size according to nonlinear convergence behavior and estimated truncation errors. This approach ensured numerical stability while resolving strong thermal and hydraulic transients in the porous and fractured media considered. The fully coupled equations were solved using a Newton–Raphson method combined with the MUMPS direct linear solver, which efficiently handled the large sparse systems arising from the 3D finite-element discretization. Nonlinear solver tolerances were set to strict values (relative tolerance on the order of 10^{-3} to 10^{-4}), and appropriate stabilization techniques were enabled to avoid oscillations in advection-dominated regions. These numerical settings provided a robust and accurate framework for the coupled TH simulations performed in this work.

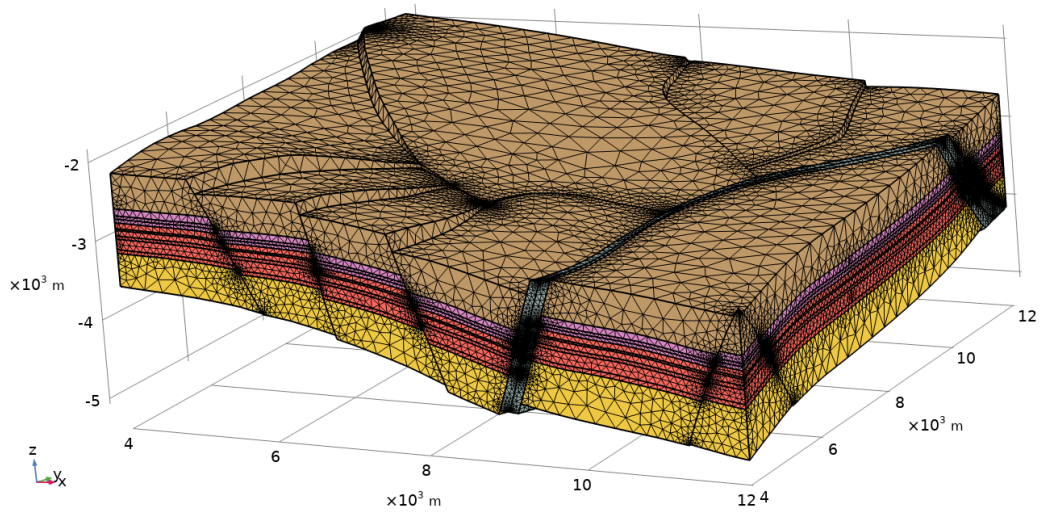


Figure 5. 3D volumetric, unstructured finite-element mesh of the reservoir model extracted from the regional 3D framework. The fault damage zone (FDZ) along the main fault—shown in blue—represents the primary target of the study, while the underlying and overlying aquitards are depicted in yellow and light brown, respectively.

4 PRELIMINARY SIMULATION RESULTS

As for the study of the factors controlling anomalously high temperature in the MUR region, several 2D vertical cross-sections were extracted from the GeORG model and the boundary conditions (BCs) were varied as to how to understand the impact of the BCs on the temperature field. This would contribute to accurately constraint the BCs for the 3D reservoir model. After implementing the prescribed initial and boundary conditions for the exploratory setup, the model was allowed to evolve over an initial timespan of 10,000 years. The outcomes—summarized in Figure 6—demonstrate several important behaviors in the thermal regime and fluid circulation across the simulated two-dimensional cross section. The principal observations include: (1) Lateral movement of high-temperature fluids is directed predominantly along an east–west trend within the basement units, (2) thermally buoyant fluids originating in the basement rise and infiltrate the stratigraphic successions above it, (3) within the Triassic reservoir formations, small-scale convection systems arise, likely controlled by internal heterogeneity and contrasts in permeability, (4) in the central region of the model domain, concentrated vertical pathways develop, expressed as distinct thermal plumes ascending through the Tertiary reservoirs.

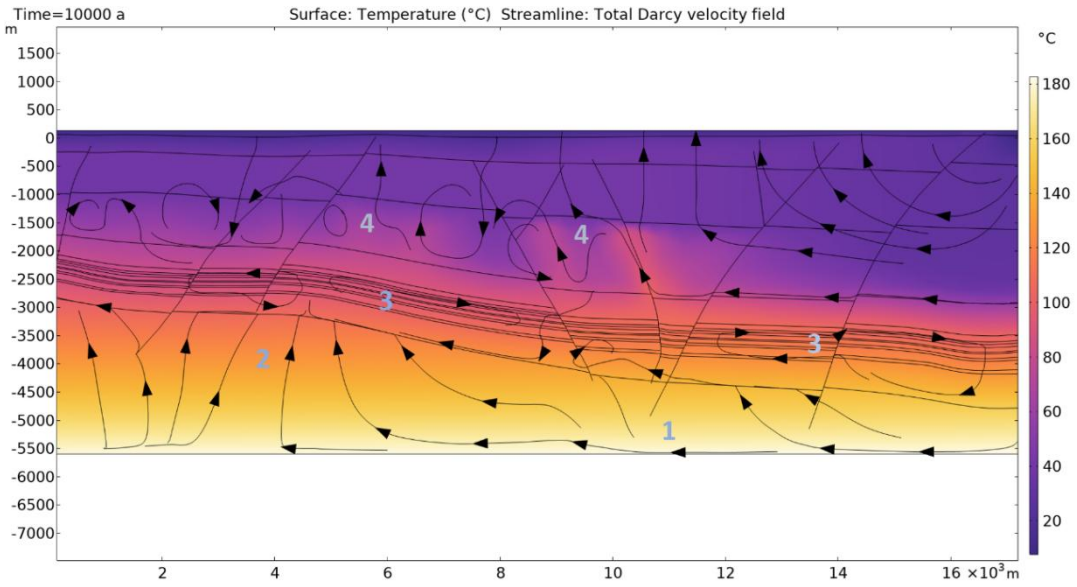


Figure 6. Temperature distribution and Darcy velocity vectors of the complex model after 10^4 years of simulation. The results highlight: (1) east–west groundwater flow along the basement interface, (2) upward migration of heated fluids from depth, (3) localized convective circulation within the Triassic units, and (4) the development of thermal plumes rising into the Tertiary reservoirs.

To assess the controls on the onset of natural convection and the extent of the thermally as well as the order of fluid velocities, we setup a 3D generic model of 5.5 x 5.5 km lateral dimensions expanding until 6 km depth that contains an inclined normal fault dipping ca. 70° in the middle of the modelling domain. Simulation results reveal important information on the interplay between permeability structure and topographic or density-driven flow. Diverse permeability structures for the FDZ and adjacent sedimentary layers were tested in conjunction with different EoS. As a matter of example, modelling outcomes in Fig. 7 show the extent of the convection cells and fluid velocity range depending on the magnitude and structure of permeability.

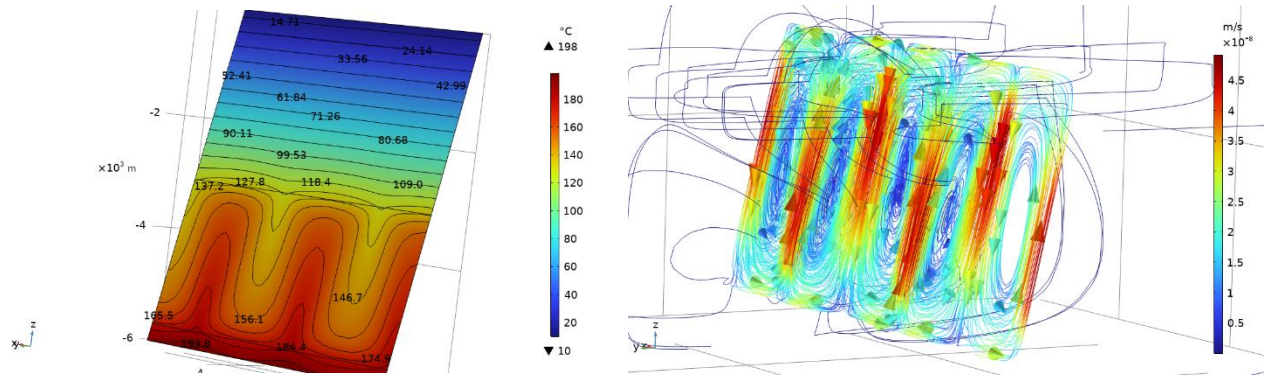


Figure 7. Simulation results for a generic 3D model (5.5 × 5.5 × 6 km) containing a 200-m-thick normal fault damage zone (FDZ) at the domain center after 250,000 years, when the system approaches quasi-steady-state conditions. Left: temperature field showing the convection-cell pattern along the fault plane. Right: corresponding fluid-velocity field. Fault permeability is set to 10^{-14} m², whereas adjacent sedimentary units are treated as tight. Hydraulic no-flow boundary conditions are applied at the lateral and basal boundaries, with atmospheric pressure imposed at the surface. Thermal insulation is assigned to the lateral boundaries, while the top and bottom boundaries are fixed at 10 °C and 0.10 W m^{-2}, respectively.

In this phase of project development, we develop several scenarios of reservoir development based on the relatively coarse GeORG model as explained previously. For a fault-controlled reservoir, the optimal position of geothermal doublets, which have to be placed within the FDZ, can be investigated using different layouts and positioning of the injection and production wells (see Fig. 8). Simulation results demonstrate the sustainability of the reservoir development during operation over 30 years since maximum pressure difference from the initial conditions are in the order of 12 bar and no thermal breakthrough is observed.

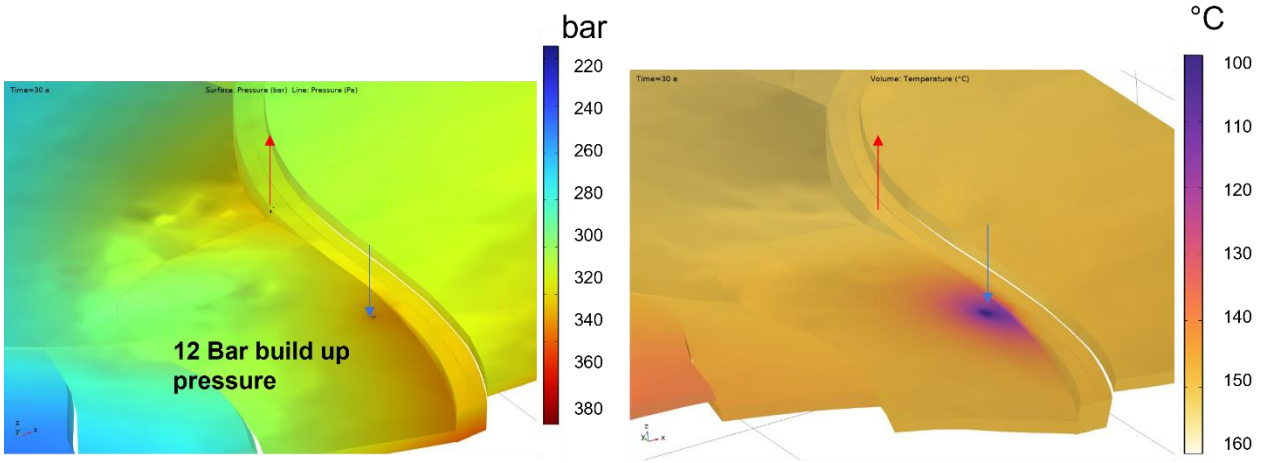


Figure 8. Preliminary simulation results for the fault damage zone shown in Fig. 5, illustrating a geothermal doublet with an injection well (blue arrow) and a production well (red arrow) separated by ~1700 m after 30 years of operation. Left: pressure field for an injection/production rate of 50 L s^{-1}. Right: temperature field for an injection temperature of 60 °C. No thermal breakthrough occurs under the assumed fault-damage-zone permeability. The geological framework is based on the GeORG model.

5 CONCLUSIONS

In representative 2D thermo-hydraulic models derived from the real-world GeORG framework, diverse convection structures emerged within 10,000 years of simulated time, largely governed by the heterogeneous permeability architecture and the topography and buoyancy driven flows. These initial findings provide the foundation for the next steps of the study. Upcoming developments will aim to enhance the 2D setup by extending the simulation period to 500,000 years, integrating the fault damage zone configuration already tested in the simplified 3D model, and widening the lateral extent to account for the influence of major boundary faults of the graben. Moreover, transitioning to a fully three-dimensional real-world representation will be a key objective, as this will allow us to assess how flow aligned with the main axis of the Upper Rhine Graben shapes the emergence and spatial distribution of thermal anomalies.

A thermo-hydraulic reservoir model was developed by extracting and refining a subset of the regional-scale model (GeORG model). Multiple scenarios were simulated over a 30-year period to evaluate reservoir performance under various geothermal doublet configurations, using a flow rate of 50 L s^{-1} and an injection temperature of 60 °C. The results indicate that the tested operational schemes remain sustainable over the simulated timeframe. Overall, the 3D TH reservoir model provides a robust tool for assessing alternative well layouts and operating strategies, as well as for conducting uncertainty analyses related to key petrophysical parameters.

The recently completed 3D seismic campaign, together with the forthcoming data from drilling and logging activities, field-based hydraulic tests, and laboratory core-flooding experiments, will substantially improve and validate the reservoir model. These combined datasets will provide critical constraints on subsurface properties and processes, thereby advancing our understanding of the anomalously high temperature distribution in the Middle Upper Rhine Region.

Acknowledgements

This work has been conducted within the framework of the DEKAPALATIN-BERTHA joint geothermal research project, which is funded by the Federal Ministry for Economic Affairs and Energy (BMWE), grant number: 03EXP4005B. We gratefully acknowledge AspenTech Subsurface Science & Engineering for providing an academic/research license for Aspen SKUA, which made the 3D static modeling and visualization of our structural and stratigraphic models possible.

REFERENCES

Abreu-Torres, J., Hutka, G., Blöcher, G., Cacace, M., Magnenet, V., and Schmittbuhl, J.: Large-scale reservoir modeling of the Vendenheim geothermal site (France), *Adv. Geosci.*, 65, 117–125 (2025).

Agemar, T., Schellschmidt, R., and Schulz, R.: Subsurface temperature distribution in Germany, *Geothermics*, 44, 65–77 (2012).

Agemar, T.; Weber, J.; Schulz, R. Deep Geothermal Energy Production in Germany. *Energies* (2014), *7*, 4397-4416.

Appelo, C. A. J., and Postma, D.: *Geochemistry, Groundwater and Pollution*, 2nd ed., A. A. Balkema Publishers, Leiden, (2005).

Böcker, J., Littke, R., and Förster, A.: An overview on source rocks and the petroleum system of the central Upper Rhine Graben, *International Journal of Earth Sciences*, 106, 707–742 (2017).

Clauser, C., and Villinger, H.**:** Analysis of conductive and convective heat transfer in a sedimentary basin, demonstrated for the Rheingraben, *Geophys. J. Int.*, 100, (1990), 393–414.

Clauser, C., Griesshaber, E., and Neugebauer, H. J.: Decoupled thermal and mantle helium anomalies: Implications for the transport regime in continental rift zones, *Journal of Geophysical Research*, 107, B11, (2002), 2269.

Diamond, L. W., and Alt-Epping, P.: Predictive modelling of mineral scaling, corrosion and the performance of solute geothermometers in a granitoid-hosted enhanced geothermal system, *Applied Geochemistry*, 51, 216–228 (2014).

Frey, M., Bär, K., Stober, I., Reinecker, J., van der Vaart, J., and Sass, I.: Assessment of deep geothermal research and development in the Upper Rhine Graben, *Geothermal Energy*, 10, No. 18, (2022).

Freymark, J., Sippel, J., Scheck-Wenderoth, M., Bär, K., Stiller, M., Fritsche, J.-G., and Kracht, M.: The deep thermal field of the Upper Rhine Graben, *Tectonophysics*, 694, (2017), 114–129.

GeORG-Projectteam, Geopotenziale des tieferen Untergrundes im Oberrheingraben, Fachlich-Technischer Abschlussbericht des INTERREG-Projekts GeORG, Teil 2: Geologische Ergebnisse und Nutzungsmöglichkeiten, Freiburg im Breisgau, Germany, (2013).

Guillou-Frottier, L., Carré, C., Bourgine, B., Bouchot, V., and Genter, A.: Structure of hydrothermal convection in the Upper Rhine Graben as inferred from corrected temperature data and basin-scale numerical models, *Journal of Volcanology and Geothermal Research*, 256, (2013), 29–49.

Guillou-Frottier, L., Duwiquet, H., Launay, G., Taillefer, A., Roche, V., and Link, G.: On the morphology and amplitude of 2D and 3D thermal anomalies induced by buoyancy-driven flow within and around fault zones, *Solid Earth*, 11, 1571–1595 (2020).

Kassem, M. A., and Moscariello, A.: Geothermal energy: A sustainable and cost-effective alternative for clean energy production and climate change mitigation, *Sustainable Future*, 10, 101247 (2025).

Koltzer, N., Scheck-Wenderoth, M., Cacace, M., Frick, M., and Bott, J.: Regional hydraulic model of the Upper Rhine Graben, *Adv. Geosci.*, 49, 197–206, (2019).

Koltzer, N., Kommana, G., Cacace, M., Frick, M., Bott, J., und Scheck-Wenderoth, M.: Influences of hydraulic boundary conditions on the deep fluid flow in a 3D regional model (central Upper Rhine Graben), *Environmental Earth Sciences*, 81(32), (2022).

Lemgruber-Traby, A., Bossennec, C., Béthune, G., Souque, C., Divies, R., van der Vaart, J., Bär, K., and Sass, I.: Basin-scale 3D modelling of the northern Upper Rhine Graben: insights into basement fault-related geothermal flow pathways, *Geoenergy*, 1(1), (2023), geoenergy2023-002.

Magri, F., Bayer, U., Maiwald, U., Otto, R., and Thomsen, C.: Impact of transition zones, variable fluid viscosity and anthropogenic activities on coupled fluid-transport processes in a shallow salt-dome environment, *Geofluids*, 9, 182–194 (2009).

Moeck, I.S.: Catalog of geothermal play types based on geologic controls, *Renewable and Sustainable Energy Reviews*, 37, (2014), 867–882.

Moeck, I. S., Franz, M., Koelbel, T., Höhn, O., Ravidà, D. C. G., Hernandez, F., Ahrens, J., Exuzian, G. L., and Erb, M.: Application of the play type approach for the federal exploration initiative in Germany – criteria catalogue and case studies, *Proceedings of the World Geothermal Congress 2026*, Calgary, Canada, June 8–11, (2026).

Nardi, A., Idiart, A., Trinchero, P., de Vries, L. M., and Molinero, J.: Interface COMSOL–PHREEQC (iCP), an efficient numerical framework for the solution of coupled multiphysics and geochemistry, *Computers & Geosciences*, 69, 10–21 (2014).

Pribnow, D., and Schellschmidt, R.: Thermal tracking of upper crustal fluid flow in the Rhine Graben, *Geophysical Journal International*, 2000, Vol.27, No. 13, 1957–1960.

Reinhold, C., Schwarz, M., Bruss, D., Heesbeen, B., Perner, M., and Suana, M.: The Northern Upper Rhine Graben – Re-dawn of a mature petroleum province? *Swiss Bulletin of Applied Geology*, 21(2), (2016), 35–56.

Sanjuan, B., Millot, R., Dezayes, C., and Brach, M.: Main characteristics of the deep geothermal brine (5 km) at Soultz-sous-Forêts (France) determined using geochemical and tracer test data, *Comptes Rendus Geoscience*, 342, (2010), 546–559.

Sanjuan, B., Millot, R., Innocent, C., Dezayes, C., Scheiber, J., and Brach, M.: Major geochemical characteristics of geothermal brines from the Upper Rhine Graben granitic basement with constraints on temperature and circulation, *Chemical Geology*, 428, (2016), 27–47.

Vallier, B., Magnenet, V., Schmittbuhl, J., and Fond, C.: Large scale hydro-thermal circulation in the deep geothermal reservoir of Soultz-sous-Forêts (France), *Geothermics*, 78, (2019), 154–169.

Xiao, Y., Whitaker, F., Xu, T., and Steefel, C. (Eds.): *Reactive Transport Modeling: Applications in Subsurface Energy and Environmental Problems*, Wiley, First published 25 March 2018.

Yanaze, T., Yoo, S., Marumo, K., and Ueda, A.: Prediction of permeability reduction due to silica scale deposition with a geochemical clogging model at Sumikawa Geothermal Power Plant, *Geothermics*, 79, 114–128 (2019).